New Application of PAS for *In Situ* Observation of Semiconductor Electrode Surface

Hideki MASUDA, Akira FUJISHIMA,* and Kenichi HONDA

Department of Synthetic Chemistry, Faculty of Engineering, The University of Tokyo, Hongo, Bunkyo-ku, Tokyo 113

(Received July 15, 1981)

The photoacoustic spectroscopic technique was used to study *in situ* cathodic decomposition of CdS and ZnO semiconductor electrodes and electrochemical deposition of metal ions (Cd^{2+} and Zn^{2+}) on the semiconductor electrodes.

Photoacoustic spectroscopy (PAS) has recently been emphasized as an useful tool for the study of materials.[1-4] In particular, absorption spectra of highly absorbing materials can easily be obtained by the PAS technique. Additionally, thermal conductivity[5] and information regarding to radiationless processes[6,7] can be obtained from photoacoustic effects. Although PAS has extensively been used to study solids, gases, and liquids,[8] application to *in situ* studies of electrode surface is just beginning. In previous publications,[9,10] we reported that change in a few monolayers on electrode surface during anodic oxidation of a gold electrode could easily be detected *in situ* by the PAS technique.

We report here an application of PAS to *in situ* measurement of semiconductor electrode reactions. Specifically, cathodic reactions of n-type semiconductor electrodes (CdS, ZnO) and electrochemical deposition of metal ions (Cd^{2+}, Zn^{2+}) from solution on electrodes are studied.

These reactions were studied by Kolb *et al.*[11,12] by use of differential reflectance spectroscopy, in which mechanically polished surfaces were examined because the surface had to be flat for this technique.

Experimental

The photoacoustic cell, shown in Fig. 1, was constructed of stainless steel and its outside surface was coated with an epoxy resin for the purpose of insulation from the electrolyte.

An electret condenser microphone (SONY Model ECM-150), a pressure transducer, was mounted on the PAS cell. It was favorable for electrochemical study because a high voltage power source was not required. A Pyrex window was situated at the other side of the cell which was directly across the sample electrode, so that the light which was not absorbed by the sample electrode could pass through the window.

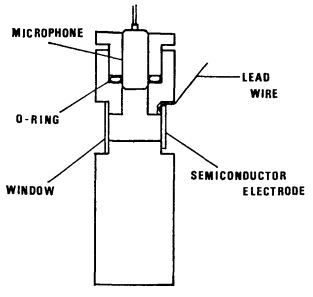

Fig. 1. Photoacoustic cell for semiconductor electrode. The cell width is 20 mm and the height is 60 mm.

Samples measured in this work were a single crystal CdS $(000\bar{1})$ [Teikoku Tsushin (with a donor concentration $N_D = 1.6 \times 10^{16}$ cm^{-3})] and a sintered polycrystalline ZnO which was made with the same procedure as described before.[13] The donor concentration of the polycrystalline ZnO was not known.

Because the amplitude of the photoacoustic signal depends on the thickness of the sample, especially for semiconductors which have lower thermal conductivities than metals, the samples were polished to a thin plate with thickness of less than 0.5 mm.

Ohmic contact was established by evaporating indium on the rear surface of the semiconductor plate, and a lead wire was contacted to the sample with Ag epoxy. Each surface of the samples, CdS and ZnO, was etched with concentrated hydrochloric acid for a few seconds prior to measurement.

The experimental instrumentation was similar to those described previously for the metal electrode-PAS measurement.[9,10] In the present work, a Rhodamin 6G dye laser (Spectra Physics Model 375) which has a wavelength range of approximately 550—660 nm, was used as a high intensity monoenergetic light source in addition to an argon ion laser (Spectra Physics Model 164) and a Xe lamp (Ushio, 1 kW). The light beam from lasers was magnified by a convex lens (f=5 cm) so that the entire surface of the sample electrode except the region of the lead wire contact could be irradiated.

Before a PAS spectrum was taken, the phase angle was adjusted so that the photoacoustic signal due to light absorption at the surface could be optimized. Excitation sources of energy corresponding to the absorption band regions of CdS and ZnO, respectively, were used during the phase adjustment. This procedure was repeated whenever the thickness of samples or modulation frequency was varied.

Results and Discussion

CdS Single Crystal Electrode. Figure 2 shows the photoacoustic signal of the CdS electrode *versus* the wavelength of excitation before and after electrolysis (about 100 mC cm^{-2}) at −2.0 V *vs.* SCE in 1 M KCl (1 M=1 mol dm^{-3}) solution.

In the spectrum of CdS before electrolysis, the photoacoustic signal began to increase when the excitation energy approached the absorption band edge of CdS (2.4 eV or 520 nm). When the energy of radiation is comparable to the band gap energy of the semiconductor electrode, electrons are excited into the conduction band, and when there is no current flow, electrons will recombine with holes in the valence band, and heat will be dissipated.

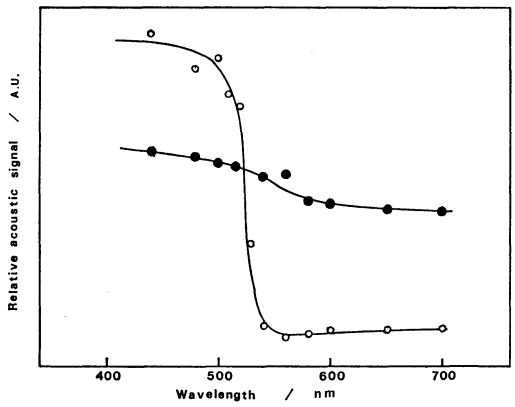

Fig. 2. Photoacoustic spectra of the CdS electrode before (—○—) and after (—●—) electrolysis at −2.0 V *vs.* SCE in 1 M KCl.

When the CdS electrode was electrolyzed at −2.0 V, decomposition of the electrode occurred as follows:

$$CdS + 2e^- \longrightarrow Cd + S^{2-}.$$

The decomposition potential was found to be −1.5 V in the dark. The surface of the CdS was covered with a deposited thin metallic layer of Cd. The photoacoustic signal in the longer wavelength region was due to the intrinsic absorption of the metallic Cd layer. There was a small increase in the photoacoustic signal beginning at an energy corresponding to the absorption band edge of CdS. This extra signal was probably due to the absorption by the CdS underneath the thin metallic Cd layer.

Based on the wavelength response of the photoacoustic signals, we used photons of two different wavelengths, one longer than (610 nm) and the other comparable to (514.5 nm) the absorption band edge of CdS, to prove surface change of the CdS electrode during a reduction and oxidation cycle.

Figure 3 shows the current-potential curve and the relative photoacoustic signal-potential curve of the CdS electrode in 1 M KCl electrolyte solution. The irradiation wavelength was 610 nm. At this wavelength, no photoeffect occurred at the CdS electrode. In the current-potential curve, during the first scan, reduction of oxygen at an onset potential of −0.9 V and hydrogen evolution at an onset potential of −1.4 V were observed, but no cathodic decomposition peak was observed because of the large cathodic current of hydrogen evolution. However, the photoacoustic signal began to increase at −1.5 V. This increase in the photoacoustic signal was due to an increase in the absorption of light at the electrode surface. The increase in the absorption of light reflected the basic change in the absorptivity of the electrode surface and was due to the Cd deposition from lattice at −1.5 V. The photoacoustic signal was not influenced by the oxygen reduction or the hydrogen evolution in the sensitivity region of the present study.

On the anodic scan, a sharp anodic peak appeared at −0.7 V in the current-potential curve, and could be attributed to the dissolution of Cd. At the corresponding potential, the photoacoustic signal decreased and finally returned to its initial value. This behavior suggests that the deposited Cd layer is completely stripped off after an anodic scan.

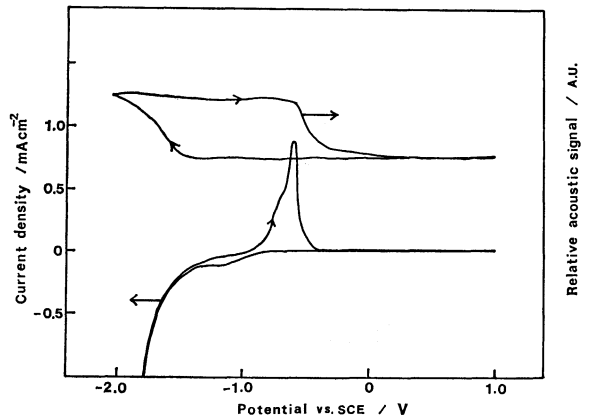

Fig. 3. Photoacoustic signal-potential and current-potential curves of the CdS electrode in 1 M KCl. Potential sweep rate: 40 s/V; λ=610 nm (Rh-6G dye laser irradiation).

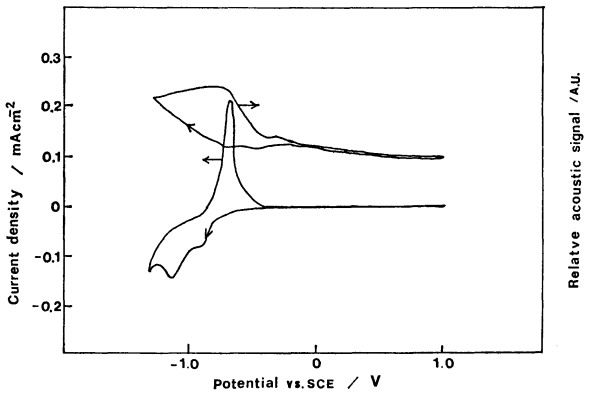

Fig. 4. Photoacoustic signal-potential and current-potential curves of the CdS electrode in the presence of 5×10^{-5} M Cd^{2+} and 1 M KCl.
Potential sweep rate: 40 s/V; λ=610 nm (Rh-6G dye laser irradiation).

Figure 4 shows the current-potential and the photoacoustic signal-potential curves of the CdS electrode in 1 M KCl solution containing 5×10^{-5} M Cd^{2+}. The potential was scanned between 1.0 and −1.4 V, and in this potential range the decomposition of CdS did not take place. A cathodic current at −0.8 V in the current-potential curve was due to the reduction of Cd^{2+} from solution on the CdS surface, thus causing the photoacoustic signal to increase.

Assuming that the deposited layer was uniform, the thickness of the deposited layer was estimated to be about 7 Å from the amount of the charge passed for the electrochemical deposition and the density of Cd (8.7 g cm^{-3}).

We could also detect a change of the CdS electrode surface during the cathodic decompositon by use of the intrinsic absorption wavelength of irradiation (514.5 nm). Figure 5 shows the current-potential and photoacoustic signal-potential curves in 1 M KCl solution using 514.5 nm irradiation. At this wavelength, the anodic photoeffect took place remarkably

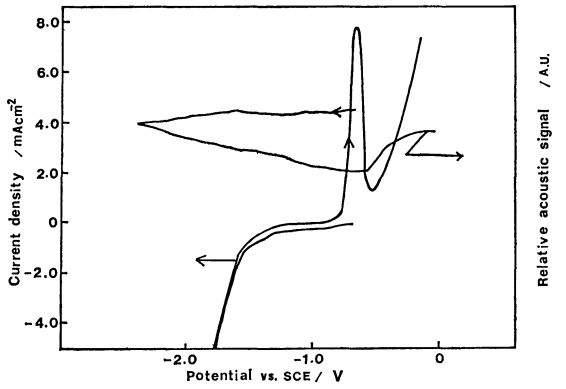

Fig. 5. Photoacoustic signal-potential and current-potential curves of the CdS electrode in 1 M KCl. Potential sweep rate: 50 s/V; λ=514.5 nm (Ar ion laser irradiation).

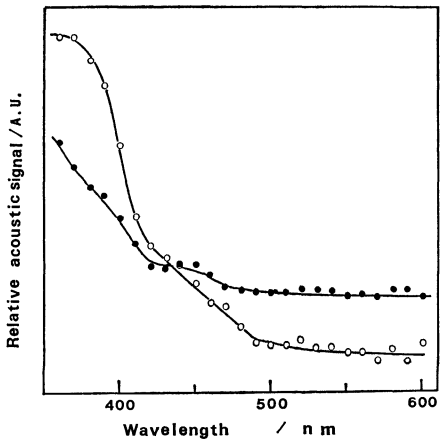

Fig. 6. Photoacoustic spectra of the ZnO electrode before (—○—) and after electrolysis (—●—) at —1.6 V in 1 M KCl.

but the cathodic did negligibly. As was expected, the photoacoustic signal was larger when there was no Cd present on the CdS surface because of the intrinsic absorption of CdS at this wavelength, as shown in Fig. 2. The photoacoustic signal began to decrease at —1.5 V where the CdS decomposition took place. This decrease in signal was due to the Cd deposition. However, the change in the photoacoustic signal was less obvious when the 514.5 nm irradiation was used.

ZnO Polycrystalline Electrode. Photoacoustic spectra of the ZnO electrode before and after electrolysis at —1.6 V (about 100 mC cm^{-2}) in 1 M KCl are shown in Fig. 6. On cathodic polarization, the ZnO electrode decomposed and a deposited Zn layer was formed as follows:

$$ZnO + 2H^+ + 2e^- \longrightarrow Zn + H_2O.$$

After electrolysis the spectra changed, that is, the absorption in the longer wavelength region increased due to deposition of Zn from the ZnO lattice. Because the metallic zinc layer was not uniformly deposited on the surface in the case of polycrystalline ZnO, the absorption of ZnO remained in the spectrum after electrolysis.

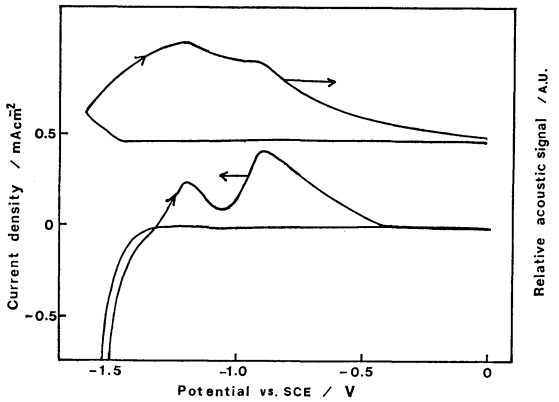

Fig. 7. Photoacoustic signal-potential and current-potential curves of the ZnO electrode in 1 M KCl. Potential sweep rate: 60 s/V; $\lambda \geqq 600$ nm (Xe lamp irradiation with a sharp cut filter).

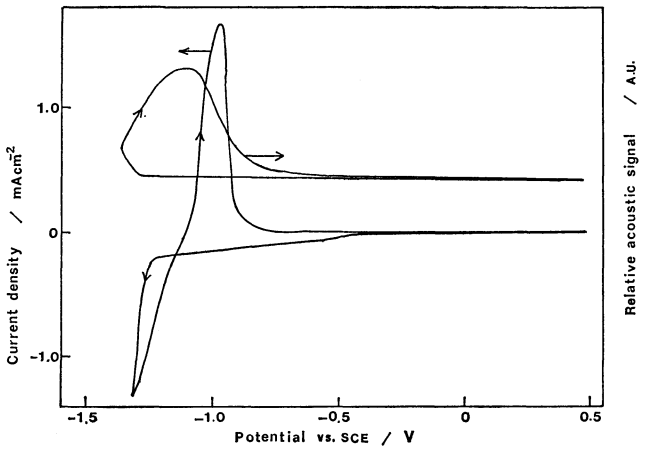

Fig. 8. Photoacoustic signal-potential and current-potential curves of the ZnO electrode in the presence of 10^{-3} M Zn^{2+}, and 1 M KCl.
Potential sweep rate: 30 s/V; $\lambda \geqq 600$ nm (Xe lamp irradiation with a sharp filter).

Figure 7 shows the photoacoustic signal under irradiation at λ>600 nm (Xe lamp irradiation) and current-applied potential curves for ZnO in 1 M KCl electrolyte. The photoacoustic signal began to increase at —1.5 V, which implied decomposition of ZnO. On the anodic scan, two anodic current peaks, both of which seemed to be attributed to dissolution of Zn layer to the solution, were observed in the current-potential curve. The photoacoustic signal decreased stepwise at the corresponding potentials. The photoacoustic signal did not return to the initial value even after the anodic scanning. This behavior implied that the deposited zinc layer could not completely dissolve and remained partially on the polycrystalline ZnO surface.

Figure 8 shows the photoacoustic signal and current-potential curves in 1 M KCl solution containing 10^{-3} M Zn^{2+} ion. A reduction current between —0.5 and —1.25 V was due to the reduction of dissolved oxygen, which did not affect the PAS signal. However, when the large cathodic current flowed from —1.25 V which was attributed to the electrochemical

deposition of Zn^{2+} on the ZnO surface from the solution, the photoacoustic signal began to increase at almost the same potential. On the anodic scan, the anodic current peak was observed at −1.0 V and the photoacoustic signal decreased from −1.1 V. In this case, only one steep peak was observed. Though detailed characters of the two kinds of metallic zinc in the cathodic decomposition (in Fig. 7) are unknown, the results relating to the current-potential and optical measurements of the ZnO in this work are in accord with those by Kolb *et al.*[11,12]

Conclusion

We have demonstrated that photoacoustic spectroscopy is surface sensitive and applicable to *in situ* characterization of the semiconductor electrode surface change during a reduction and oxidation cycle. We could detect deposition of several layers of metal using laser irradiation. This technique is simple and useful for studies of rough or porous surfaces. The problem that the sample has to be thin in our method might be solved by use of other techniques, *e.g.* the piezoelectric photoacoustic detection technique.[14–16] Application of PAS to photoelectrochemical reactions of semiconductor electrodes was described elsewhere.[17]

The authors would like to thank Dr. Boon H. Loo at SRI International for his valuable suggestions.

References

1) A. Rosencwaig, *Opt. Commun.*, **7**, 305 (1973).
2) A. Rosencwaig, *Anal. Chem.*, **47**, 592A (1975).
3) W. R. Harshburger and M. B. Robin, *Acc. Chem. Res.*, **6**, 329 (1973).
4) M. J. Adams, A. A. King, and G. F. Kirkbright, *Analyst*, **101**, 73 (1976).
5) M. J. Adams and G. F. Kirkbright, *Analyst*, **102**, 281 (1977).
6) J. C. Murphy and L. C. Aamodt, *J. Appl. Phys.*, **48**, 3502 (1977).
7) R. G. Peterson and R. C. Powell, *Chem. Phys. Lett.*, **53**, 366 (1978).
8) See for example, Technical Digest, Topical Meeting on Photoacoustic Spectroscopy, Ames., Iowa (1979).
9) A. Fujishima, H. Masuda, and K. Honda, *Chem. Lett.*, **1979**, 1063.
10) H. Masuda, A. Fujishima, and K. Honda, *Bull. Chem. Soc. Jpn.*, **53**, 1542 (1980).
11) D. M. Kolb and H. Gerischer, *Electrochim. Acta*, **18**, 987 (1973).
12) D. M. Kolb, *Ber. Bunsenges. Phys. Chem.*, **77**, 891 (1973).
13) T. Inoue, A. Fujishima, and K. Honda, *J. Electrochem. Soc.*, **127**, 1582 (1980).
14) M. M. Farrow, R. K. Burnham, M. Avzanneau, S. L. Olsen, N. Purdie, and E. M. Eyring, *Appl. Opt.*, **17**, 1093. (1978).
15) W. Jackson and N. M. Amer, *J. Appl. Phys.*, **51**, 3343 (1980).
16) R. E. Malpas and A. J. Bard, *Anal. Chem.*, **52**, 109 (1980).
17) H. Masuda, S. Morishita, A. Fujishima, and K. Honda, *J. Electroanal. Chem.*, **122**, 67 (1981).